

Two and Three-Dimensional CT Mapping of Hoffa Fractures

Xuetao Xie, MD, PhD*, Yu Zhan, MD*, Minjie Dong, MD, Qifang He, MD, Justin F. Lucas, MD, Yingqi Zhang, MD, PhD, Yukai Wang, MD, and Congfeng Luo, MD

Investigation performed at the Shanghai Sixth People's Hospital, Shanghai Jiaotong University School of Medicine, Shanghai, China

Background: Hoffa fractures, coronal-plane fractures involving the distal femoral condyles, are unstable, intra-articular fractures. The aim of this study was to define the location and frequency of fracture lines and comminution zones in Hoffa fractures using computed tomography (CT) mapping in both 2-dimensional and 3-dimensional contexts.

Methods: Seventy-five Hoffa fractures (OTA/AO types 33B3.2 and 33B3.3) were retrospectively reviewed. The directions of fracture lines were characterized in the axial and sagittal CT planes. CT images for all fractures were superimposed on one another and oriented to fit a standard template. Mapping of fracture lines and comminution zones in both the axial and sagittal planes was performed. A 3-dimensional map was created by reducing reconstructed fracture fragments to fit to a model of the distal aspect of the femur.

Results: This study included 1 bicondylar and 74 unicondylar (26 medial and 48 lateral) Hoffa fractures. Comminuted fractures accounted for 35.5% of all fractures and 44.9% of lateral fractures. Axial fracture mapping demonstrated that fracture lines were concentrated in the middle-third area of the lateral condyle but were less concentrated and with greater variation in the medial condyle. The mean angle of fracture lines with respect to the posterior condylar axis was 34.4° and 29.0° in the lateral and medial femoral condyles, respectively. Sagittal fracture mapping also demonstrated that fracture lines were concentrated in the middle third of the lateral condyle but were less concentrated in the medial condyle. The mean angle of fracture lines with respect to the posterior cortex of the distal femoral shaft was 23.1° and 19.3° in the lateral and medial condyles, respectively. Three-dimensional mapping demonstrated comminution zones commonly occurring in the weight-bearing zone of the lateral condylar articular surface.

Conclusions: Hoffa fractures occurred more frequently in the lateral femoral condyle. In the axial plane, fractures commonly extended from anterolateral to posteromedial in the lateral condyle and from anteromedial to posterolateral in the medial femoral condyle. In the sagittal plane, fractures traversed from anteroinferior to posterosuperior. Articular comminution was more commonly seen in lateral condylar fractures and concentrated in the weight-bearing zone of the articular surface.

Clinical Relevance: Research in this area is imperative for optimal preoperative planning, such as for the selection of surgical approach and fixation constructs. Our findings lend insight into fracture morphology, which can assist with fracture classification and the design of biomechanical studies, ultimately aiding in treatment.

Hoffa fractures, coronal-plane fractures involving the distal femoral condyles, are unstable, intra-articular fractures that can occur either in isolation or as a component of more complex intra-articular injuries. They are found in either condyle but more commonly occur in the lateral condyle^{1,2}. The injury can be easily overlooked with conventional radiographic imaging, especially if nondisplaced or

when present in association with a supracondylar-intercondylar distal femoral fracture³. Computed tomography (CT) has thus been recommended to improve the diagnostic yield³⁻⁵. Nonoperative treatment of Hoffa fractures was reportedly associated with secondary displacement and poor functional results⁶. Operative treatment with anatomic reduction, rigid internal fixation, and early rehabilitation protocols has been advocated^{1,2,4-6}.

*Xuetao Xie, MD, PhD, and Yu Zhan, MD, contributed equally to the writing of this article.

Disclosure: No external funding was received for this study. The **Disclosure of Potential Conflicts of Interest** forms are provided with the online version of the article (<http://links.lww.com/JBJS/E440>).

Essential components in the successful treatment of intra-articular fractures include visualization of the articular injury and direct reduction through appropriate surgical exposure. Rigid internal fixation with an absolute-stability construct applied in a biomechanically advantageous manner facilitates the best potential for recovery. In the setting of Hoffa fractures, these components can only be achieved with a thorough understanding of the coronal-plane fracture pattern. In 1978, Letenneur et al. classified Hoffa fractures into 3 types according to the location and direction of fracture lines on lateral radiographs⁷. Since that time, however, little progress has been made to further explore and characterize Hoffa fracture morphology. As CT imaging has become, over the past decade, routine in the assessment of patients when clinical suspicion of a Hoffa fracture is present, it is now possible to discern the injury characteristics in both the 2-dimensional (2-D) and 3-dimensional (3-D) contexts.

The purpose of this study was to define the location and frequency of fracture lines and comminution zones of Hoffa fractures by means of 2-D and 3-D CT mapping techniques in addition to conventional radiographic measurements of fracture lines. We hypothesized that there are consistent fracture patterns and zones of comminution for Hoffa fractures.

Materials and Methods

Subjects

Using a prospectively maintained orthopaedic database at a large level-I trauma center, we conducted a retrospective search for the CT imaging data of patients with a diagnosis of a Hoffa fracture between December 2008 and December 2016. The OTA/AO fracture classification was used to identify isolated Hoffa fractures (type 33B3.2 for unicondylar fractures or type 33B3.3 for bicondylar fractures)⁸. The case records and imaging data concerning all type-33B fractures were also reviewed independently by 3 investigators to identify the initially

missed Hoffa fractures. Patients <18 years of age or with axial CT images with a slice thickness of >3 mm were excluded. A total of 75 Hoffa fractures in 75 patients were included. Case records were retrieved to identify concomitant injuries, particularly fractures around the knee joint.

Radiographic Analysis

Raw CT data were obtained in the axial plane and imported into Mimics software (Materialise) to create a project file. Fractures were then analyzed simultaneously in the axial, sagittal, and coronal planes, allowing for reconstruction of 3-D models. The posterior condylar axis (PCA) and the posterior cortex of the distal femoral shaft (PCF) were chosen as reference lines to reorient the CT images for standardization: (1) the axial plane was perpendicular to the PCF, and (2) the sagittal plane was perpendicular to the PCA.

The axial views that most prominently demonstrated the medial and lateral epicondyles were selected to analyze the Hoffa fracture lines. Angle α was defined as the acute angle formed by the fracture line and the PCA (Fig. 1-A). The value was positive when the fracture line ran from anterolateral to posteromedial in the lateral condyle or from anteromedial to posterolateral in the medial condyle; otherwise, negative values were obtained. The sagittal views demonstrating the largest area of the injured condyles were selected. Angle β was defined as the acute angle formed by the fracture line and the PCF (Fig. 1-B). The value was positive when the fracture line ran from anteroinferior to posterosuperior in either condyle; otherwise, negative values were obtained.

Fracture Mapping

The method of 2-D fracture mapping as described by Cole et al.⁹ and Armitage et al.¹⁰ was used in this study. Briefly, reformatted axial and sagittal views of all fractures were imported into Adobe Illustrator software to overlap one another

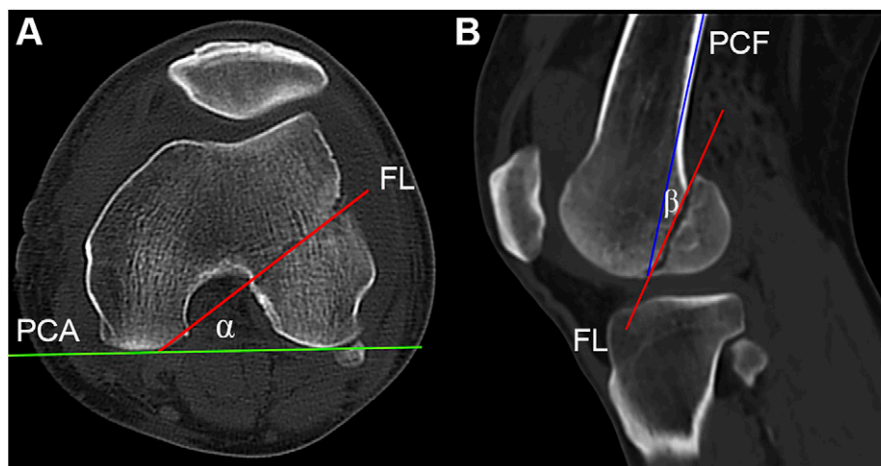


Fig. 1
Radiographic measurements of Hoffa fracture lines. **Fig. 1-A** Angle α was defined as the acute angle formed by the fracture line (FL) (red line) and the posterior condylar axis (PCA) (green line). **Fig. 1-B** Angle β was defined as the acute angle formed by the FL (red line) and the posterior cortex of the distal femoral shaft (PCF) (blue line).

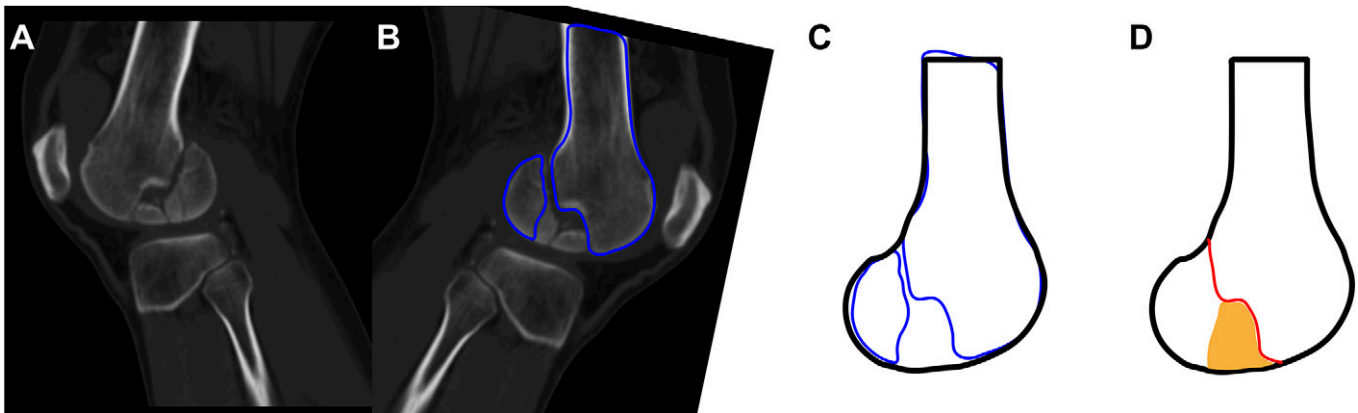


Fig. 2

The method used for 2-D CT mapping of Hoffa fractures. **Fig. 2-A** A sagittal CT image shows a displaced, comminuted Hoffa fracture in the lateral condyle. **Fig. 2-B** The sagittal image was flipped horizontally and rotated before major fragments were identified with blue lines. **Fig. 2-C** The displaced fragments were virtually reduced on the basis of a sagittal template. **Fig. 2-D** The fracture line (red line) and comminution zone (orange area) were marked on the template.

on a standard template. This resulted in a superimposed compilation of fracture lines and comminution zones on individual templates of both the axial and sagittal views of the distal aspects. Comminution zones were defined as zones with fragments of $<1 \text{ cm}^2$ area^{9,11}. Proper rotation and identification of fracture fragments were performed by aligning specific landmarks: the medial and lateral epicondyles, the patellar groove, the intercondylar notch, and the osseous contours of the femoral condyles. Fracture lines and comminution zones were then individually reproduced on a corresponding distal femoral template (Fig. 2). The overlapping of all layers resulted in a 2-D diagram with variations in density relative to fracture frequency and comminution zones.

In order to create a 3-D frequency diagram, the Hoffa fracture fragments were reconstructed in Mimics software and virtually reduced. Data were then exported into 3-matic software (Materialise), and reconstructed fragments were rotated, normalized, and horizontally flipped, if necessary, to best match a 3-D model of the distal aspect of the femur (by Y.Z.). Smooth curves were drawn directly on the surface of the model to delineate the fracture lines and to mark the comminution zones of each case (Fig. 3). An analysis of the overlap of

all fracture lines and comminution zones allowed for the production of a 3-D Hoffa fracture map. Details of the 3-D mapping technique are provided in the Appendix.

Data Analysis

Patient characteristics and fracture measurements are summarized as the mean and standard deviation or the proportion. A comparison between the medial and lateral condyles with respect to the categorical data was performed using GraphPad Prism 6.0 with chi-square or Fisher exact tests, if appropriate. A p value of <0.05 was considered significant. Morphologic fracture-map analysis and characterization was descriptive in nature.

Results

Patient characteristics and radiographic measurements of the Hoffa fractures are summarized in Table I. Among the 75 patients, 61 (81.3%) of the fractures occurred in patients aged 31 to 70 years, with a frequency peak among patients aged 51 to 60 years (Fig. 4). Seventy-four unicondylar fractures (type 33B3.2), including 48 lateral and 26 medial fractures, and 1 bicondylar fracture (type 33B3.3) were included. Comminuted

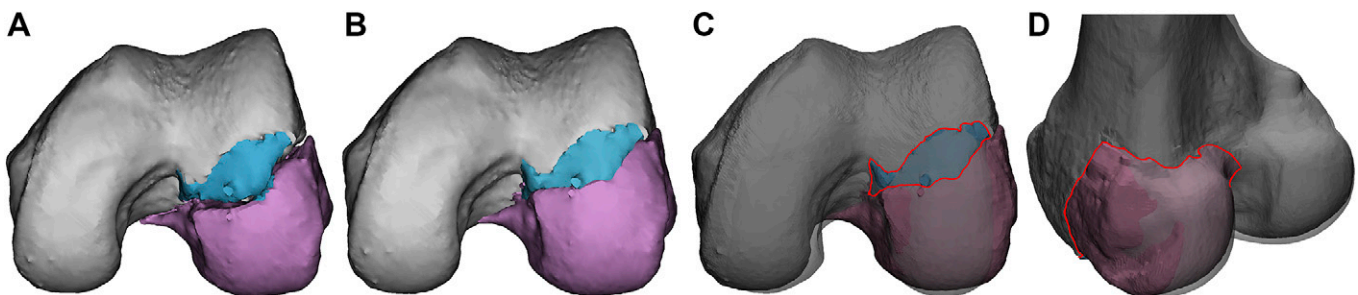


Fig. 3

The method used for 3-D CT mapping of Hoffa fractures (see also Appendix). In this example of a lateral comminuted Hoffa fracture, each fragment was reconstructed (**Fig. 3-A**) and then virtually reduced (**Fig. 3-B**). When the Hoffa fracture was fit to a 3-D model of the distal aspect of the femur, the comminution zone was identified with a red outline (**Fig. 3-C**) and the fracture line was marked with a red line (**Fig. 3-D**).

TABLE I Patient Demographics and Fracture Characteristics

	Medial Condyle	Lateral Condyle	Total
Fractures* (no. [%])	27 (35.5)	49 (64.5)	76 (100)
Age† (yr)	47.0 (20-66)	52.6 (18-80)	50.4 (18-80)
Sex‡ (no. [%])			
Male	18 (66.7)	34 (69.4)	52 (68.4)
Female	9 (33.3)	15 (30.6)	24 (31.6)
Side of injury‡ (no. [%])			
Left knee	13 (48.1)	27 (55.1)	40 (52.6)
Right knee	14 (51.9)	22 (44.9)	36 (47.4)
Fracture type‡ (no. [%])			
Simple	22 (81.5)	27 (55.1)	49 (64.5)
Comminuted	5 (18.5)	22 (44.9)	27 (35.5)
Open or closed‡ (no. [%])			
Open	2 (7.4)	0 (0)	2 (2.6)
Closed	25 (92.6)	49 (100)	74 (97.4)
Concomitant injury§ (no. [%])			
Fracture	21 (77.8)	31 (63.3)	52 (69.3)
Ipsilateral knee fracture	12 (44.4)	16 (32.7)	28 (37.3)
Ipsilateral tibial plateau fracture	5 (18.5)	14 (28.6)	19 (25.3)
Angle# (°)			
α	29.0 \pm 20.5	34.4 \pm 11.6	32.5 \pm 15.5
β	19.3 \pm 17.0	23.1 \pm 14.9	21.8 \pm 15.6

*The only case of a bicondylar Hoffa fracture, in a left knee, is represented here as 1 medial and 1 lateral condylar fracture. †The values are given as the mean, with the range in parentheses. ‡The percentage shown is of the total number of fractures within the indicated condyle or, in the final column, of the total number of fractures. §The percentage shown is of the total number of fractures within the indicated condyle or, in the final column, of the total number of patients (n = 75). #The values are given as the mean and the standard deviation.

fractures were more commonly observed in the lateral condyle (22 of 49 total fractures) than in the medial condyle (5 of 27 total fractures) ($p = 0.02$).

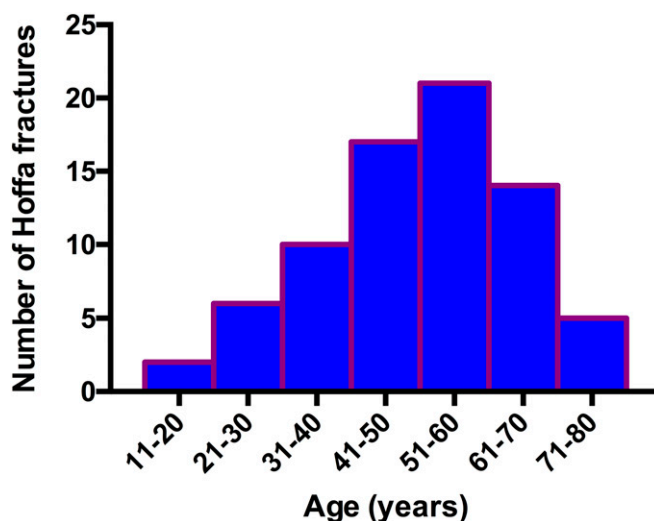


Fig. 4
The distribution of fractures by patient age.

Axial Maps

In the lateral femoral condyle, the majority of the fracture lines were concentrated in the middle-third area, with a trajectory running from anterolateral to posteromedial (Fig. 5-A). Specifically, the majority of fracture lines originated near the junction of the anterior and middle thirds laterally and exited medially on the anterior half of the lateral wall of the intercondylar notch. The mean α angle measurement was 34.4° (range, -8.4° to 52.7°), with 83.7% of the lines within 20° to 50° relative to the PCA. The comminution zones were mainly located in the central to lateral part of the middle-third area, generally in the direction of fracture lines across this area (Fig. 5-B).

Compared with those in the lateral femoral condyle, the fracture lines in the medial condyle were less concentrated through the middle-third area and found to have greater variation in trajectory (Fig. 5-A). Specifically, the majority of fracture lines were oblique, extending from anteromedial to posterolateral and exiting around the roof of the intercondylar notch; however, variation was noted, including several transverse fracture lines from medial to lateral located in the posterior third of the femoral condyle. The mean α angle measurement was 29.0° (range, -19.4° to 59.4°), with 59.3% of the lines within 20° to 50° relative to the PCA. There were

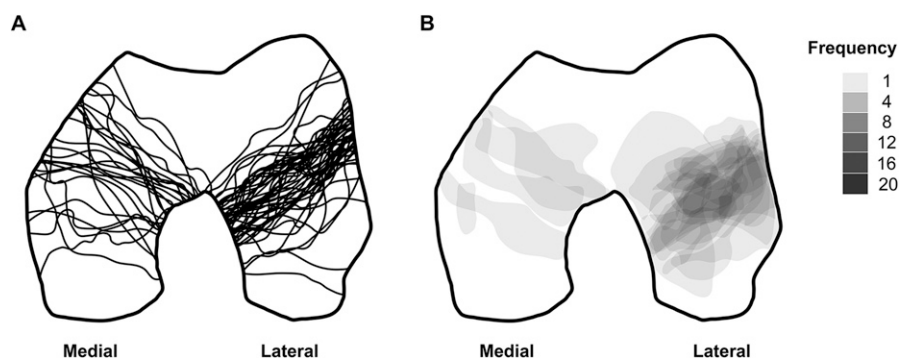


Fig. 5
Axial maps of the 75 Hoffa fractures. **Fig. 5-A** Fracture lines. **Fig. 5-B** Comminution zones. Darker colors represent higher frequency of comminution zones.

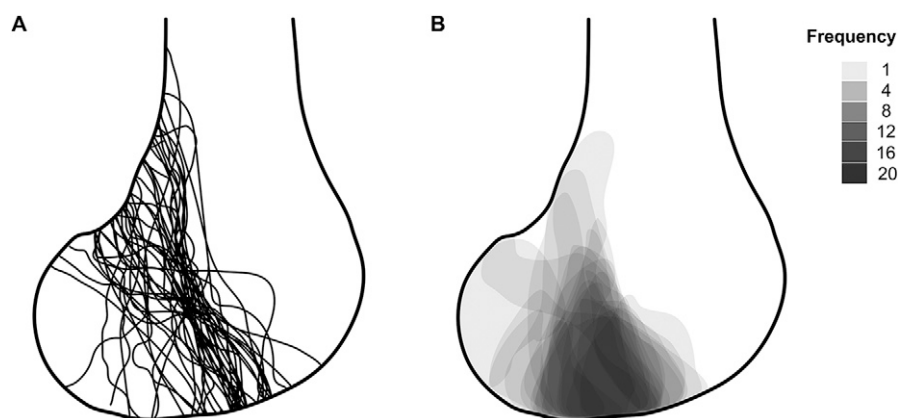


Fig. 6
Sagittal maps of the lateral Hoffa fractures. **Fig. 6-A** Fracture lines. **Fig. 6-B** Comminution zones. Darker colors represent higher frequency of comminution zones.

only 5 distinct zones of comminution, mainly distributed in the middle-third area in line with the fracture lines across this area (Fig. 5-B).

Sagittal Maps

In the lateral condyle, the majority of the fracture lines were concentrated in the middle-third area, running in an anteroinferior

to posterosuperior direction and exiting at the posterior aspect of the distal metaphysis (Fig. 6-A). The mean β angle measurement was 23.1° (range, -8.2° to 68.2°), with 73.5% of the lines within 10° to 40° relative to the PCF. The comminution zones were also frequently located in the middle-third area, forming a sector extending to the articular surface (Fig. 6-B).

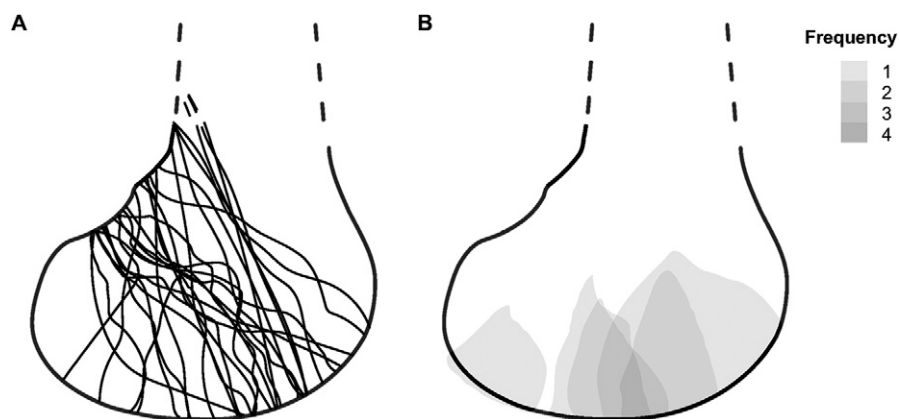


Fig. 7
Sagittal maps of the medial Hoffa fractures. The dashed lines represent the proximal extension of the condylar cortex and fractures lines not seen on the slices selected for fracture mapping. **Fig. 7-A** Fracture lines. **Fig. 7-B** Comminution zones. Darker colors represent higher frequency of comminution zones.

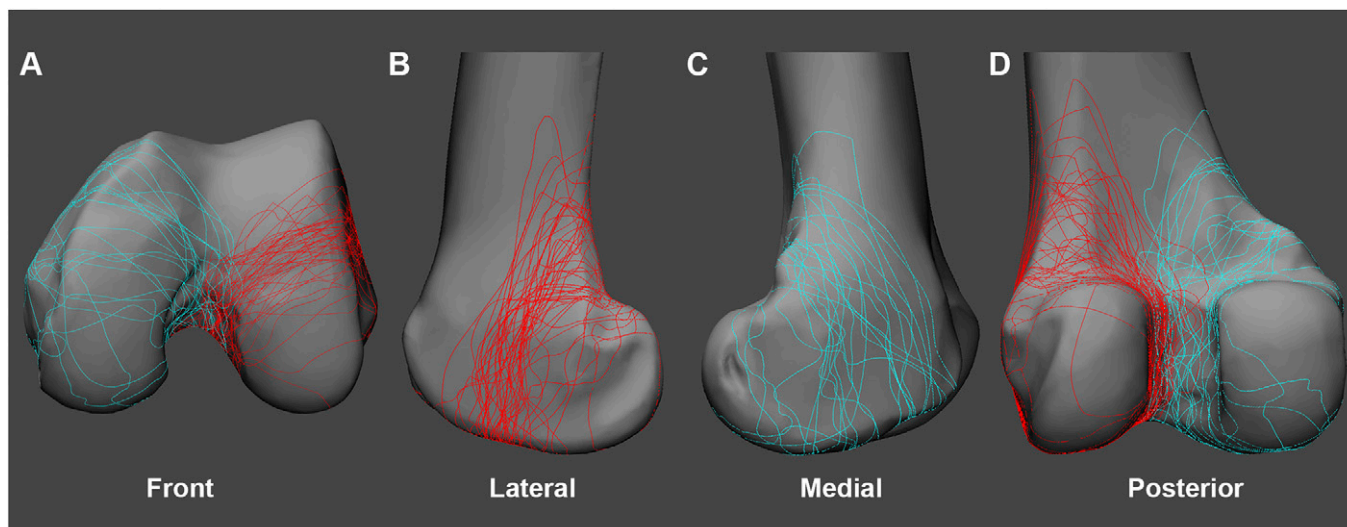


Fig. 8
Representative views of the 3-D map of the 75 Hoffa fracture lines, including front (**Fig. 8-A**), lateral (**Fig. 8-B**), medial (**Fig. 8-C**), and posterior (**Fig. 8-D**) views. Fractures are represented by cyan lines in the medial condyle and red lines in the lateral condyle.

Compared with those in the lateral femoral condyle, and similar to the results of the axial-plane analysis, fracture lines in the medial condyle on sagittal-plane analysis were less concentrated in location, despite more than half running across the middle-third area from anteroinferior to posterosuperior (**Fig. 7-A**). The mean β angle measurement was 19.3° (range, -10.8° to 58.6°), with 63% of the lines within 10° to 40° relative to the PCF. There were only 5 discrete zones of comminution identified, with an overlap located in the middle-third area (**Fig. 7-B**).

3-D Maps

In the lateral femoral condyle, the majority of the fracture lines ran in a trajectory from the anterior half of the lateral wall of the intercondylar notch, extending anterolaterally across the middle third of the tibiofemoral articular surface. On the lateral view, fracture lines progressed posterosuperiorly to the posterior aspect of the metaphyseal region. Finally, on the posterior

view, fracture lines converged into the anterior half of the intercondylar notch (**Fig. 8**; see also Video 1, which demonstrates the 3-D map of the 75 Hoffa fracture lines). By combined-plane analysis, a common fracture plane was identified, originating from the most distal articular surface of the lateral condyle and traversing posterosuperiorly and posteromedially. Comminution zones were concentrated in the central to lateral part of the middle of the tibiofemoral articular surface, an area considered to be the main weight-bearing zone of the knee joint (**Fig. 9**; see also Video 2, which demonstrates the 3-D map of the 27 comminution zones).

Fracture lines in the medial femoral condyle were found to run in a trajectory similar to that in the lateral condyle; however, they were much less concentrated in the front and medial views. On the posterior view, most fracture lines were found to converge into the roof of the intercondylar notch (**Fig. 8**; Video 1). Comminution zones were evenly dispersed throughout the weight-bearing area, with an overlap in the middle region (**Fig. 9**; Video 2).

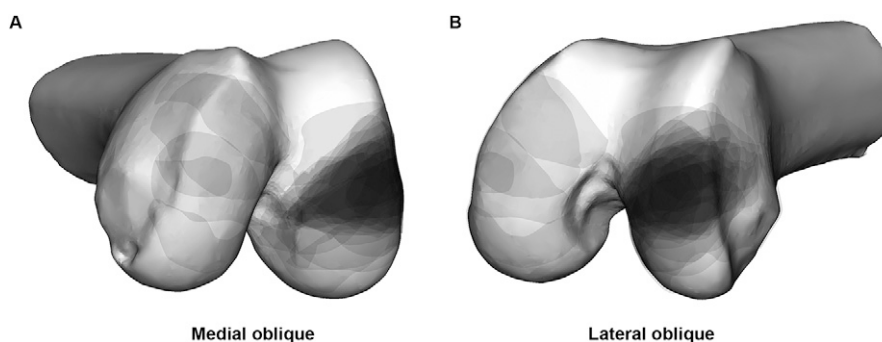


Fig. 9
Representative views of the 3-D map of the 27 comminution zones, including medial oblique (**Fig. 9-A**) and lateral oblique (**Fig. 9-B**) views. Darker colors represent higher frequency of comminution zones.

Discussion

In this study, the fracture-mapping technique described by Cole et al.⁹ and Armitage et al.¹⁰ was applied to 75 isolated Hoffa fractures, the largest number of Hoffa cases, to our knowledge, reported in a study to date, in order to improve understanding of this intra-articular injury. A quantitative evaluation method using uniquely derived fracture characteristics was developed and combined with a qualitative evaluation of fracture patterns including 2-D and 3-D analysis to provide a comprehensive description of Hoffa fragment morphology. Hoffa fractures most commonly occurred in the middle third of the lateral condyle, extending from anteroinferior to posterosuperior and from anterolateral to posteromedial. A greater amount of comminution was observed in lateral condylar fractures and was mainly concentrated in the middle-third region. Compared with the lateral condyle, fracture lines and comminution zones in the medial condyle were distributed in a less-concentrated fashion, although an overlap was generally noted within the middle-third region.

Improved understanding of Hoffa fracture morphology such as described in this study can have notable clinical impact in facilitating successful preoperative planning. In comparison with previous work³, in which the degree of comminution associated with Hoffa fragments may have been underestimated, results obtained through our method of 3-D fracture analysis demonstrated that 44.9% of lateral Hoffa fractures and 35.5% of all Hoffa fractures had a substantial amount of associated comminution. The prevalence of articular comminution suggests that traditional surgical approaches for exposure of simple fracture lines may need modification for improved visualization of the articular surface at the focal point of the zone of comminution^{12,13}. Additionally, articular comminution was found to be concentrated in the middle-third, weight-bearing zone of the condylar surface. Due to the high physiologic loads and structural demands required for stability in this region of the femoral condyle, special considerations including intraoperative bone-grafting may be warranted¹⁴. Lastly, the fixation of comminuted Hoffa fractures may be different from that of more simple fracture patterns. It was previously reported that screw fixation for simple Hoffa fractures was not sufficient in the setting of comminution but rather, such fractures were better stabilized using plate fixation with buttressing^{15,16}. Underestimation of the amount of articular comminution in Hoffa fractures during preoperative planning may lead to fixation failure¹⁶, fracture nonunion¹⁷, or malunion^{18,19}.

Hoffa fracture maps in this study can also aid in the development of a more thorough and descriptive classification system. The classification proposed by Letenneur et al. in 1978 divides Hoffa fractures into 3 types: type I, involving the entire posterior condyle and parallel to the posterior cortex; type II, also parallel to the posterior cortex but a smaller fracture; and type III, an oblique fracture⁷. This description of fracture configurations was based on an evaluation of radiographs of 20 cases, in an attempt to predict the risk of osteonecrosis⁷;

however, to our knowledge, this work has not been validated⁶. In our study, we found that fracture-line orientations were both continuous and multiplanar. There was no distinct cutoff either between the parallel (type-I or II) and oblique (type-III) fracture lines or among the condylar fragments of various sizes (type I versus type II). A subjective classification of fracture patterns into 1 of the 3 types as described by Letenneur et al. may not obtain satisfactory interobserver agreement. On the basis of the OTA/AO classification⁸, Hoffa fractures are categorized into 1 of 2 groups: unicondylar (type 33B3.2) or bicondylar (type 33B3.3). Critical morphologic details, such as fracture orientation and comminution zones, cannot accurately be reflected in this particular classification scheme. The purpose of this study was not to propose a new classification system; however, the trends present in the 2-D and 3-D fracture maps may prove useful in facilitating improved communication and surgical understanding of fixation concepts to better address the complex articular injuries.

Furthermore, the fracture patterns revealed in our study may improve the development of fixation concepts relative to Hoffa fractures. Three previous biomechanical studies investigated the strength of various screw or plate fixation methods²⁰⁻²². All of the studies simulated simple Hoffa fractures in the lateral femoral condyle. Two simulated Letenneur type-I fractures parallel to the posterior cortex^{20,21}, while the third did not describe the fracture orientation²². According to our study, the most common Hoffa fractures were neither parallel to the PCF in the sagittal plane, nor parallel to the PCA in the axial plane. In addition, none of the previous 3 studies investigated the fixation of segmental or comminuted fractures, which we found were not uncommon among Hoffa fractures. With a more accurate understanding of Hoffa fracture morphology, further biomechanical studies can thus be conducted that better simulate injury patterns experienced in the clinical setting.

To our knowledge, this is the first study to elucidate the common fracture patterns and articular comminution of isolated Hoffa fractures by means of 2-D and 3-D fracture mapping techniques in combination with radiographic measurements. Fracture mapping in 2 dimensions has been widely used to improve the understanding of injury patterns in a variety of bones, including extra-articular scapular fractures¹⁰, tibial plateau fractures¹¹, and pilon fractures⁹. While 3-D mapping is time-consuming and technically demanding, it is considered to be more accurate in the demonstration of fracture morphology in comparison with 2-D mapping²³ and provides additional information imperative for preoperative planning. In this study, the 3-D Hoffa fracture maps illustrated the surface anatomy of common fracture lines and articular comminution, which could be explored to design the optimal surgical approach to best expose the fractures and minimize the risk of injury of key structures in the vicinity. Although the depth of articular comminution could be reflected on the sagittal 2-D maps, the 3-D maps illustrated the anatomical location and surface area. Therefore, 2-D maps showed the “inside” of the


fractures, whereas 3-D maps display the “outside” of the fractures; combining the 2 techniques can enhance the completeness and accuracy of our understanding of Hoffa fractures.

There were some limitations of this study. First, coronal-plane fractures associated with supracondylar, intercondylar, or complete articular fractures were not included in this case series. It was reported that 38.1% of 202 supracondylar-intercondylar distal femoral fractures (type 33C) were diagnosed in association with coronal-plane fractures, with 66% of these fractures being open³. Direct inclusion of these fractures in this study might have resulted in a more thorough spectrum of Hoffa fracture patterns; however, the increased complexity would have made the current fracture-mapping techniques difficult to apply and the results more difficult to interpret. Moreover, the treatment regimen, including the surgical approach, fragment reduction, and fixation method, is also different between more complex distal femoral fractures (type 33C)²⁴ and isolated Hoffa fractures (type 33B3.2 and type 33B3.3)⁴. Another limitation was that the morphologic evaluation of Hoffa fractures in this study was based on CT imaging. The fracture maps may not have been representative of missed Hoffa fractures or those that were diagnosed without CT imaging. Nork et al. previously reported that only 69% of 95 coronal-plane fragments were diagnosed with use of biplanar radiographs³. Since these findings in 2005, CT has become a routine tool in our department in the setting of clinical suspicion of Hoffa fractures.

In conclusion, the data presented have elucidated common patterns of isolated Hoffa fractures in the form of a series of 2-D and 3-D Hoffa fracture maps in combination with radiographic measurements. The middle third of the lateral femoral condyle was predisposed to Hoffa fractures and a substantial amount of articular comminution. In the axial plane, fractures commonly extended from anterolateral

to posteromedial or from anteromedial to posterolateral in lateral and medial femoral condylar fractures, respectively. Fractures traversed from antero-inferior to posterosuperior in the sagittal plane, with comminution, if present, localized to the weight-bearing zone of the femoral condyle.

Appendix

 Details of the 3-D mapping technique, including 2 figures, are available with the online version of this article as a data supplement at [jbjs.org \(http://links.lww.com/JBJS/E441\)](http://links.lww.com/JBJS/E441). ■

Xuetao Xie, MD, PhD¹

Yu Zhan, MD¹

Minjie Dong, MD²

Qifang He, MD¹

Justin F. Lucas, MD³

Yingqi Zhang, MD, PhD⁴

Yukai Wang, MD¹

Congfeng Luo, MD¹

¹Department of Orthopaedic Surgery, Shanghai Sixth People's Hospital, Shanghai Jiaotong University School of Medicine, Shanghai, China

²Department of Orthopaedic Surgery, Changzheng Hospital Affiliated to Second Military Medical University, Shanghai, China

³Department of Orthopedic Surgery, University of California, Davis, Sacramento, California

⁴Department of Orthopaedic Surgery, Tongji Hospital, Tongji University School of Medicine, Shanghai, China

E-mail address for C. Luo: congfenl@outlook.com

ORCID iD for C. Luo: [0000-0001-5876-5266](https://orcid.org/0000-0001-5876-5266)

References

- Gavaskar AS, Tummala NC, Krishnamurthy M. Operative management of Hoffa fractures—a prospective review of 18 patients. *Injury*. 2011 Dec;42(12):1495-8. Epub 2011 Oct 10.
- Dhillon MS, Mootha AK, Bali K, Prabhakar S, Dhatt SS, Kumar V. Coronal fractures of the medial femoral condyle: a series of 6 cases and review of literature. *Musculoskelet Surg*. 2012 Jun;96(1):49-54. Epub 2011 Sep 9.
- Nork SE, Segina DN, Aflatoon K, Barei DP, Henley MB, Holt S, Benirschke SK. The association between supracondylar-intercondylar distal femoral fractures and coronal plane fractures. *J Bone Joint Surg Am*. 2005 Mar;87(3):564-9.
- Arastu MH, Kokke MC, Duffy PJ, Korley RE, Buckley RE. Coronal plane partial articular fractures of the distal femoral condyle: current concepts in management. *Bone Joint J*. 2013 Sep;95-B(9):1165-71.
- White EA, Matcuk GR, Schein A, Skalski M, Marecek GS, Forrester DM, Patel DB. Coronal plane fracture of the femoral condyles: anatomy, injury patterns, and approach to management of the Hoffa fragment. *Skeletal Radiol*. 2015 Jan;44(1):37-43. Epub 2014 Oct 2.
- Lewis SL, Pozo JL, Muirhead-Allwood WF. Coronal fractures of the lateral femoral condyle. *J Bone Joint Surg Br*. 1989 Jan;71(1):118-20.
- Letenneur J, Labour PE, Rogez JM, Lignon J, Bainvel JV. [Hoffa's fractures. Report of 20 cases (author's transl)]. *Ann Chir*. 1978 Mar-Apr;32(3-4):213-9. French.
- Marsh JL, Slongo TF, Agel J, Broderick JS, Creevey W, DeCoster TA, Prokuski L, Sirkin MS, Ziran B, Henley B, Audigé L. Fracture and dislocation classification compendium - 2007: Orthopaedic Trauma Association Classification, Database and Outcomes Committee. *J Orthop Trauma*. 2007 Nov-Dec;21(10)(Suppl):S1-133.
- Cole PA, Mehrle RK, Bhandari M, Zlowodzki M. The pilon map: fracture lines and comminution zones in OTA/AO type 43C3 pilon fractures. *J Orthop Trauma*. 2013 Jul;27(7):e152-6.
- Armitage BM, Wijdicks CA, Tarkin IS, Schroder LK, Marek DJ, Zlowodzki M, Cole PA. Mapping of scapular fractures with three-dimensional computed tomography. *J Bone Joint Surg Am*. 2009 Sep;91(9):2222-8.
- Molenaars RJ, Mellema JJ, Doornberg JN, Kloen P. Tibial plateau fracture characteristics: computed tomography mapping of lateral, medial, and bicondylar fractures. *J Bone Joint Surg Am*. 2015 Sep 16;97(18):1512-20.
- Taitzman LA, Frank JB, Mills WJ, Barei DP, Nork SE. Osteochondral fracture of the distal lateral femoral condyle: a report of two cases. *J Orthop Trauma*. 2006 May;20(5):358-62.
- Viskontas DG, Nork SE, Barei DP, Dunbar R. Technique of reduction and fixation of unicondylar medial Hoffa fracture. *Am J Orthop (Belle Mead NJ)*. 2010 Sep;39(9):424-8.
- Mahadevan D, Challand C, Keenan J. Depressed femoral condyle fracture. *Inj Extra*. 2008 Jan;39(1):30-3.
- Soni A, Sen RK, Saini UC, Singh D, Chaudhary S. Buttress plating for a rare case of comminuted medial condylar Hoffa fracture associated with patellar fracture. *Chin J Traumatol*. 2012;15(4):238-40.

- 16.** Cheng PL, Choi SH, Hsu YC. Hoffa fracture: should precautions be taken during fixation and rehabilitation? *Hong Kong Med J*. 2009 Oct;15(5):385-7.
- 17.** Somford MP, van Ooij B, Schafoth MU, Kloen P. Hoffa nonunion, two cases treated with headless compression screws. *J Knee Surg*. 2013 Dec;26(Suppl 1):S89-93. Epub 2012 Jul 13.
- 18.** Iwai T, Hamada M, Miyama T, Shino K. Intra-articular corrective osteotomy for malunited Hoffa fracture: a case report. *Sports Med Arthrosc Rehabil Ther Technol*. 2012 Aug 7;4(1):28.
- 19.** Sasidharan B, Shetty S, Philip S, Shetty S. Reconstructive osteotomy for a malunited medial Hoffa fracture - a feasible salvage option. *J Orthop*. 2016 Mar 26;13(3):132-5.
- 20.** Jarit GJ, Kummer FJ, Gibber MJ, Egol KA. A mechanical evaluation of two fixation methods using cancellous screws for coronal fractures of the lateral condyle of the distal femur (OTA type 33B). *J Orthop Trauma*. 2006 Apr;20(4):273-6.
- 21.** Sun H, He QF, Huang YG, Pan JF, Luo CF, Chai YM. Plate fixation for Letenneur type I Hoffa fracture: a biomechanical study. *Injury*. 2017 Mar 30:S0020-1383(17)30198-5. Epub 2017 Mar 30.
- 22.** Hak DJ, Nguyen J, Curtiss S, Hazelwood S. Coronal fractures of the distal femoral condyle: a biomechanical evaluation of four internal fixation constructs. *Injury*. 2005 Sep;36(9):1103-6.
- 23.** Dugarte AJ, Tkany L, Schroder LK, Petersik A, Cole PA. Comparison of 2 versus 3 dimensional fracture mapping strategies for 3 dimensional computerized tomography reconstructions of scapula neck and body fractures. *J Orthop Res*. 2017 May 19. [Epub ahead of print].
- 24.** Gwathmey FW Jr, Jones-Quaidoo SM, Kahler D, Hurwitz S, Cui Q. Distal femoral fractures: current concepts. *J Am Acad Orthop Surg*. 2010 Oct;18(10):597-607.